Article | Received 13 November 2023; Accepted 20 March 2024; Published 8 April 2024
https://doi.org/10.55092/aias20240002

An input-dependent safety measure and fail-safe strategy for multicopters

Gen Cui[1,2], Guangxun Du[1,2], Quan Quan[2,*], Zhiyu Xi[2], Yang Liu[2] and Kai-Yuan Cai[2]

[1]Information Science Academy, China Electronics Technology Group Corporation, Beijing 100041, China
[2]School of Automation Science and Electrical Engineering, Beihang University, Beijing 100191, China

* Correspondence author; E-mail: qq_buaa@buaa.edu.cn.

Abstract: In order to prevent loss of control (LOC) accidents, the real-time safety measure problem is studied for multicopters. Unlike the existing work, this paper does not try to monitor the performance of the controllers by system states. In turn, the lumped disturbances of multicopters under off-nominal conditions on input are estimated to affect a proposed measure to show users whether a multicopter will be LOC. Firstly, a new degree of controllability (DoC) is proposed for multicopters subject to control constraints and off-nominal conditions. An input-dependent safety measure is then defined based on the new DoC to show the control performance for multicopters to ensure safety. Besides, the proposed measure is applied to a fail-safe strategy to guide the control decision of multicopter under off-nominal conditions. Finally, simulation and experimental results show the effectiveness of the proposed measure and fail-safe strategy.

Keywords: multicopters; loss of control; safety measure; degree of controllability; health evaluation

1. Introduction

Multicopters have attracted increasing attention in recent years [1, 2]. Due to their excellent and unique characteristics, they have been applied in numerous fields, such as surveillance, inspection, and mapping. Applications of large multicopters are becoming even more eye-catching, while they have more potential risks than microcopters if they crash unexpectedly [3]. Therefore, the problems about flight safety and how to prevent accidents due to loss of control (LOC) have attracted the attention of researchers and engineers worldwide [4–6]. Therefore, more and more researchers have been focusing on related areas like fault-tolerant control (FTC) [7, 8], *etc*.

Current multicopter autopilots are primarily designed for operations or missions under nominal conditions (e.g., a predefined weight distribution, good multicopter health, and acceptable wind disturbances). However, it is inevitable to encounter off-nominal conditions (e.g., additional payloads, propulsor degradation, and unacceptable wind disturbances). Thus, it is essential to find a proper way to evaluate the health and safety of a multicopter under off-nominal conditions. Based on the evaluation results, an appropriate fail-safe strategy [1] (chapter 14) that will not worsen the situation can then be performed. Therefore, a proper safety measure is necessary to tell users or autopilots whether the multicopter is still working well under off-nominal conditions.

Safety measure, or health evaluation in other words, is a very important topic, as evidenced by the reviews in [9, 10] and the references therein. Unlike fault diagnosis, health evaluation does not merely focus on the state of some specific components but the whole system. Furthermore, the evaluation result is not just "OK" or "Failed" but a more quantitative and comprehensive index. To be exact, health evaluation refers to the process of judging whether the system is working correctly and whether there is an anomaly or a potential failure during a certain period in the future [1] (chapter 14). In the field of aircraft, such a process is essential to guarantee safety.

Generally, the ways we may adopt are various. For example, in [11], the health state of a fixed-wing aircraft is evaluated by quantifying the permissible flight envelope with robust tracking performance. In [12], prognostic tools are developed to evaluate the propulsion system's health state to detect the onset of electrical failures in an aircraft power generator.

In this paper, an input-dependent control safety measure is proposed based on that new kind of degree of controllability (DoC) [13]. Some explanations are made in the following.

(1) Why DoC. The concept of controllability is first proposed in [14] and then extended to DoC. It is often applied when designing or analysising the properties of a system, such as actuator placement [15] and control performance improvement [16]. In recent years, the DoC of a system under disturbance has been receiving attention [17, 18]. So, a straightforward idea comes up naturally to take all the uncertainties, failures, and faults as a lumped disturbance and estimating the DoC. It may serve as an indicator of the performance of the system. Intuitively, the performance is improved as the resulting DoC increases, and vice versa. The new kind of DoC adopted in this paper for multicopters is defined based on the available control authority index (ACAI) [13]. Generally, most works for DoC do not take the effect of external disturbances and control constraints into account directly, while the ACAI does. Compared with existing DoCs, the new DoC has the following advantages: independent of the recovery time, considers the control constraints, and can reflect the effect of the disturbances.

(2) Why input-dependent. Compared with the more commonly used state-based DoC, recovery time is unnecessary for the input-dependent DoC. Recovery time is the time that a system takes to return its initial system state to origin and DoC usually varies as it changes. For the input-dependent DoC, the recovery time is unnecessary, which is illustrated in Section 3. Besides, the input-dependent DoC can be estimated onboard in real-time, while the former needs to be computed offline. Also, compared with the state-dependent controllable region, the proposed method is easy to implement because the disturbance with four control variables is only lumped and easy to estimate.

In other words, we do not monitor the safety state concerning system states. Instead, lumped disturbances of multicopters under off-nominal conditions are estimated to yield a proposed measure that tells the user whether the multicopter will be LOC. The method is easy to use because only some basic physical parameters of the multicopter and estimated disturbances are needed. By the way, the DoC can also be used as an indicator of the fault recoverability of the UAV system, which is also quite an important topic [19].

The major contributions of this paper are as follows.

i. Based on the DoC, the paper defines an input-dependent safety measure that reflects the safety margin of multicopters. This measure considers the estimated disturbances caused by off-nominal conditions on the input of the multicopter.
ii. The proposed safety measure is applied to a fail-safe strategy, which guides the control decision of the multicopter under off-nominal conditions. This strategy aims to prevent loss of control accidents and ensure the safety of the multicopter.
iii. The effectiveness of the proposed measure and fail-safe strategy is demonstrated through simulation and experimental results. These results show the practical effectiveness of the measure in monitoring the real-time safety state of multicopters and notifying users about the safety of operation.

The remainder of this paper is organized as follows. The dynamic model of a multicopter is introduced first of all (Section 2.). A step-by-step procedure is then presented to obtain the proposed measure (Section 3.). The proposed measure is applied to a fail-safe strategy to tell the user/autopilot whether the multicopter is safe or working well (Section 4.). Finally, the effectiveness of the new measure is demonstrated by both numerical and real experiments (Section 5.).

2. Problem formulation

2.1. *Mathematical model of multicopters*

Consider a multicopter with a rigid frame equipped with n_P propellers. In practice, the multicopter uses all the n_P propellers to generate the total thrust, denoted by u_t, and control torques, denoted by τ_x, τ_y, and τ_z.

Let $\mathscr{I} = \{\mathbf{e}_x, \mathbf{e}_y, \mathbf{e}_z\}$ denote the right-hand inertial frame, and $\mathscr{A} = \{\mathbf{e}_1, \mathbf{e}_2, \mathbf{e}_3\}$ denote the (right-hand) body fixed frame rigidly attached to the aircraft where the center of gravity (CoG) of the multicopter is chosen as the origin of $\mathscr{A}$.

According to [13] and [20], the mapping from the thrust $f_i, i = 1, \cdots, n_P$ to the thrust and torque vector $\mathbf{u}_f \triangleq \begin{bmatrix} u_t & \tau_x & \tau_y & \tau_z \end{bmatrix}^{\mathrm{T}}$ is given by $\mathbf{u}_f = \mathbf{B}_f \mathbf{f}$, where $\mathbf{f} \triangleq \begin{bmatrix} f_1 & f_2 & \cdots & f_{n_P} \end{bmatrix}^{\mathrm{T}}$, and $\mathbf{B}_f = \begin{bmatrix} \mathbf{b}_1^{\mathrm{T}} & \mathbf{b}_2^{\mathrm{T}} & \mathbf{b}_3^{\mathrm{T}} & \mathbf{b}_4^{\mathrm{T}} \end{bmatrix}^{\mathrm{T}} \in \mathbb{R}^{4 \times n_P}$ is the control effectiveness matrix. The linear approximate model of a multicopter is given by [1]

$$\begin{cases} \dot{h} = v_h \\ m_a \dot{v}_h = m_a g - u_t + d_u \\ \dot{\Theta} = \boldsymbol{\omega} \\ \mathbf{J} \dot{\boldsymbol{\omega}} = \mathbf{u}_\tau + \mathbf{d}_\tau \end{cases} \tag{1}$$

where m_a and $\mathbf{J} \triangleq \mathrm{diag}(J_x, J_y, J_z) \in \mathbb{R}^{3 \times 3}$ denote the mass and inertia matrix of the multicopter, respectively. g denotes the gravitational acceleration, v_h denotes the velocity of the origin of $\mathscr{A}$ with respect to $\mathscr{I}$ along the $\mathbf{e}_z$ axis, $\Theta \triangleq \begin{bmatrix} \phi & \theta & \psi \end{bmatrix}^{\mathrm{T}}$ denotes the angles of roll, pitch, and yaw, and $\boldsymbol{\omega} \triangleq \begin{bmatrix} p & q & r \end{bmatrix}^{\mathrm{T}}$ denotes the angular velocities of the frame $\mathscr{A}$ with respect to $\mathscr{I}$.

The model (1) is quite simple after linearization with small-angle approximation. The choice of modeling the attitude with Euler's angles may not allow a good description of the dynamics when a multicopter flips or does other strenuous actions. However, we lack enough tools to analyze such a comprehensive but strong nonlinear model. Instead, analyzing the approximate model (1) with all kinds of classic tools primarily developed for linear time-invariant (LTI) systems is much easier. But, of course, the final result in the following sections shows that our method still works well under real circumstances.

In model (1), the terms d_u and $\mathbf{d}_\tau \triangleq \begin{bmatrix} d_l & d_m & d_n \end{bmatrix}^{\mathrm{T}} \in \mathbb{R}^3$ are both time-variant and used to denote the unknown disturbances and the other high order nonlinear terms, such as additional payloads, propulsor degradation, external disturbances, or unmodeled dynamics. To be exact,

i. Additional payloads will change the mass m_a and inertia $\mathbf{J}$ of the multicopter.
ii. Propulsor degradation will change the control effectiveness matrix $\mathbf{B}_f$ to $\mathbf{E} \triangleq \mathbf{B}_f (\mathbf{I}_{n_P} - \boldsymbol{\Gamma}) \in \mathbb{R}^{4 \times n_P}$, where $\boldsymbol{\Gamma} \triangleq \mathrm{diag}(\eta_1, \cdots, \eta_{n_P}) \in \mathbb{R}^{n_P \times n_P}$ and $\eta_i \in [0,1], i = 1, \cdots, n_P$ denote propulsor efficiency degradation. If the i-th propulsor fails, then $\eta_i = 1$. Subsequently, propulsor degradation will introduce additional the term $\mathbf{B}_f \boldsymbol{\Gamma} \mathbf{f}$.
iii. Wind disturbance will also affect the dynamics of multicopters.

2.2. *Abstract model of multicopters*

A basic controller for multicopter, as shown in Figure 1, usually consists of an altitude controller, attitude controllers (including the roll, pitch, and yaw), and a control allocation module. In practice, PID algorithms are usually used for each controller (see [1] (chapter 11) for more details). The pseudo-inverse matrix method is usually used for the control allocation module, which is given as follows:

$$\mathbf{f} = \mathbf{B}_f^{\mathrm{T}} \left(\mathbf{B}_f \mathbf{B}_f^{\mathrm{T}} \right)^{-1} \mathbf{u}_f. \tag{2}$$

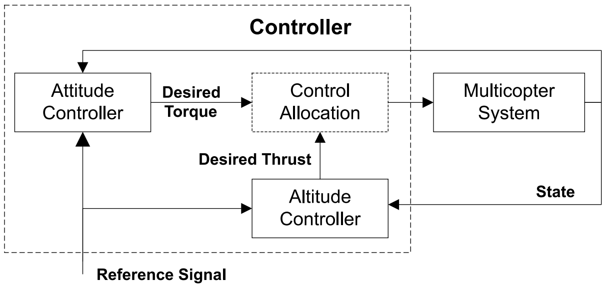

Figure 1. A multicopter control system.

Generally, the multicopter works under nominal conditions, and its controller can keep the system outputs following the desired reference signals. Things could be different under some severe conditions, for example, the complete loss of one propulsor. In [21,22], a new degraded control strategy was proposed for safety consideration, and the authors can stabilize the flight even though the yaw angle control is lost. That is, by attempting to maintain the current altitude and the multicopter attitude except for the yaw state, we can try to land the multicopter safely. In this case, a simpler 3-DoF (Degree of Freedom) model of the original system should be adopted without the degree of yaw.

If things worsen again and the maximum lift of the propulsion system becomes smaller than the gravity due to damage, then we may need to make the last choice. It is impossible to maintain altitude anymore, and what the controller can do now is to keep the pitch and roll angle to zero to avoid flipping and causing more severe damage. A 2-DoF model of the original system should be adopted in this case.

Here, no matter what mode the multicopter is in, the dynamics of the above systems can be formulated as follows:

$$\begin{aligned} &\dot{\mathbf{x}} = \mathbf{A}\mathbf{x} + \mathbf{B}(\mathbf{u} - \mathbf{d}), \quad \mathbf{u} = \mathbf{H}\boldsymbol{\mu} \\ &\mathbf{A} = \begin{bmatrix} \mathbf{0}_n & \mathbf{I}_n \\ \mathbf{0}_n & \mathbf{0}_n \end{bmatrix}, \qquad \mathbf{B} = \begin{bmatrix} \mathbf{0}_n \\ \mathbf{M}^{-1} \end{bmatrix}, \end{aligned} \tag{3}$$

where $\mathbf{x} \in \mathbb{R}^{2n}$, $\boldsymbol{\mu} \in \mathscr{U} \subset \mathbb{R}^m$, $\mathbf{u} \in \Omega \subset \mathbb{R}^n$, $\mathbf{d} \in \mathbb{R}^n$, $\mathbf{M} \in \mathbb{R}^{n \times n}$, and $\mathbf{H} \in \mathbb{R}^{n \times m}$.

- For linear 4 DoF system, one has

$$\begin{aligned} &n = 4, m = n_P, \boldsymbol{\mu} \triangleq \mathbf{f}, \mathbf{d} \triangleq \begin{bmatrix} d_u + g & -\mathbf{d}_\tau^{\mathrm{T}} \end{bmatrix}^{\mathrm{T}}, \\ &\mathbf{x} \triangleq \begin{bmatrix} h & \phi & \theta & \psi & v_h & p & q & r \end{bmatrix}^{\mathrm{T}}, \\ &\mathbf{H} \triangleq \mathbf{B}_f, \mathbf{M} \triangleq \mathrm{diag}\left(-m_a, J_x, J_y, J_z\right). \end{aligned} \tag{4}$$

- For the 3 DoF degraded system, one has

$$\begin{aligned} &n = 3, m = n_P, \boldsymbol{\mu} \triangleq \mathbf{f}, \mathbf{d} \triangleq \begin{bmatrix} d_u + g & -d_l & -d_m \end{bmatrix}^{\mathrm{T}}, \\ &\mathbf{x} \triangleq \begin{bmatrix} h & \phi & \theta & v_h & p & q \end{bmatrix}^{\mathrm{T}}, \mathbf{M} \triangleq \mathrm{diag}\left(-m_a, J_x, J_y\right) \\ &\mathbf{H} \triangleq \mathbf{B}_{f1} = \begin{bmatrix} \mathbf{b}_1^{\mathrm{T}} & \mathbf{b}_2^{\mathrm{T}} & \mathbf{b}_3^{\mathrm{T}} \end{bmatrix}^{\mathrm{T}}. \end{aligned} \tag{5}$$

- For the 2 DoF degraded system, one has

$$\begin{aligned} & n=2, m=n_P, \boldsymbol{\mu} \triangleq \mathbf{f}, \mathbf{d} \triangleq \begin{bmatrix} -d_l & -d_m \end{bmatrix}^{\mathrm{T}}, \\ & \mathbf{x} \triangleq \begin{bmatrix} \phi & \theta & p & q \end{bmatrix}^{\mathrm{T}}, \\ & \mathbf{H} \triangleq \mathbf{B}_{f2} = \begin{bmatrix} \mathbf{b}_2^{\mathrm{T}} & \mathbf{b}_3^{\mathrm{T}} \end{bmatrix}^{\mathrm{T}}, \mathbf{M} \triangleq \operatorname{diag}\left(J_x, J_y\right). \end{aligned} \tag{6}$$

In practice, $f_i \in [0, K_i], i = 1, \cdots, n_P$ (where K_i is the maximum thrust of the i-th propulsor) because the propulsors can provide only unidirectional thrust (upward or downward). The set $\mathscr{U}$ is given by $\boldsymbol{\mu} \in \mathscr{U} \triangleq \{\mathbf{f} | f_i \in [0, K_i], i = 1, \cdots, n_P\}$. Then, one has $\mathbf{u} \in \Omega \triangleq \{\mathbf{u} | \mathbf{u} = \mathbf{H}\boldsymbol{\mu}\} \subset \mathbb{R}^n$.

2.3. *Objective*

In practice, system (3) is usually controlled by the controller given by $\mathbf{u} = C(t, \mathbf{x})$. The objective of this paper is to solve the following problems:

i. How to measure the safety of the closed-loop system with controller $\mathbf{u} = C(t, \mathbf{x})$ during the flight?
ii. How to guide users or autopilots based on the monitoring result to keep multicopters safe under severe off-nominal conditions?

3. An input-dependent safety measure for multicopters

This section proposes an input-dependent safety measure for the system (3). The corresponding results are applied to the three different models.

3.1. *Preliminaries*

To test the controllability of the disturbance-driven system (3), the ACAI-based controllability analysis method is given [13] is adopted in this paper. Before proceeding further, a function is defined as

$$\rho(\boldsymbol{\alpha}, \partial\Omega) \triangleq \begin{cases} \min\limits_{\boldsymbol{\beta} \in \partial\Omega} \|\boldsymbol{\alpha} - \boldsymbol{\beta}\|, & \boldsymbol{\alpha} \in \Omega \\ -\min\limits_{\boldsymbol{\beta} \in \partial\Omega} \|\boldsymbol{\alpha} - \boldsymbol{\beta}\|, & \boldsymbol{\alpha} \in \Omega^C \end{cases} \tag{7}$$

where $\boldsymbol{\alpha} \in \mathbb{R}^n$ is a variable, $\boldsymbol{\beta}$ is a point in Ω, $\partial\Omega$ is the boundary of Ω, and Ω^C is the complementary set of Ω. The value of $\rho(\boldsymbol{\alpha}, \partial\Omega)$ represents the relationship between $\boldsymbol{\alpha}$ and Ω, which is shown in Figure 2.

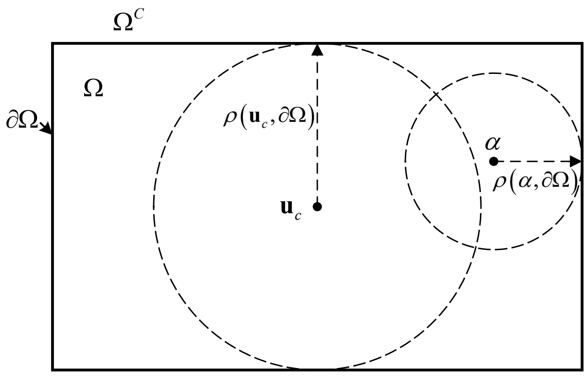

Figure 2. The schema to represent the relationship between $\boldsymbol{\alpha}$ and Ω.

$\rho(\boldsymbol{\alpha}, \partial\Omega) > 0$ implies that $\boldsymbol{\alpha}$ is an interior point of Ω. Otherwise, $\boldsymbol{\alpha}$ is not, namely $\boldsymbol{\alpha} \in \Omega^C \cup \partial\Omega$. In addition, the value of $|\rho(\boldsymbol{\alpha}, \partial\Omega)|$ represents the distance from $\boldsymbol{\alpha}$ to $\partial\Omega$. The

ACAI of system (3) is defined by the value of $\rho(\mathbf{d}, \partial\Omega) \in \mathbb{R}$, and the following theorem is given in [13].

Theorem 1. The system (3) is controllable if and only if $\rho(\mathbf{d}, \partial\Omega) > 0$.

Physically, $\rho(\mathbf{d}, \partial\Omega)$ (if $\mathbf{d} \in \Omega$) is the radius of the largest enclosed sphere centered at $\mathbf{d}$ in the attainable control set Ω (as shown in Figure 2). $\rho(\mathbf{d}, \partial\Omega) > 0$ means that $\mathbf{d}$ is an interior point of Ω. The larger the value of $\rho(\mathbf{d}, \partial\Omega)$ is, the greater the control margin a system has to reject disturbances. Specifically, if $\rho(\mathbf{d}, \partial\Omega)$ is zero, the system is trimmable, but no control margin (to trim) remains, and system LOC occurs. The value of $\rho(\mathbf{d}, \partial\Omega)$ can be taken as the trim margin of the control input $\mathbf{u}$. Obviously, controllability and trim margin typically mean different things, but the trim margin can be used somehow to measure the DoC.

3.2. An input-dependent safety measure

As mentioned above, the ACAI $\rho(\mathbf{d}, \partial\Omega)$ indicates the largest tolerance to disturbances for a multicopter. However, some things about the ACAI could still be improved. Firstly, the size of space Ω varies with different multicopters with different propulsion systems. As a result, normalization is necessary if we want to evaluate the propulsion system of multicopters. Besides, it also needs to consider the controller. For the above reasons, a new DoC is first defined, and we also need to consider the impact of different controllers.

3.2.1. Degree of controllability

Before proceeding further, a special ACAI $\rho(\mathbf{u}_c, \partial\Omega)$ is used to normalize the ACAI, where $\mathbf{u}_c = \mathbf{H}\boldsymbol{\mu}_c$ is the center of Ω and $\boldsymbol{\mu}_c = \frac{1}{2}\begin{bmatrix} K_1 & K_2 & \cdots & K_{n_P} \end{bmatrix}^{\mathrm{T}}$. The following lemma is obtained according to (7).

Lemma 1. The value $\rho(\mathbf{u}_c, \partial\Omega)$ is the maximum ACAI of system (3), let $\rho_{\max} = \rho(\mathbf{u}_c, \partial\Omega)$.

Proof: This lemma is proved geometrically. For the system (3), the direct input constraint set $\mathscr{U}$ is a high-dimensional cube. And Ω is the image of $\mathscr{U}$ after linear mapping by $\mathbf{H}$, which is a constant matrix. Therefore, the image of the center of $\mathscr{U}$ is also the center of Ω, and the image of these parallel sides of $\mathscr{U}$ are still parallel in Ω.

As shown in Figure 3, P_1P_5 and P_2P_4 are an arbitrary pair of parallel sides, P_i is an interior of Ω, and P_1P_2 and P_4P_5 are two perpendiculars to the pair of sides and they pass points $\mathbf{u}_c$ and P_i respectively. Let $\beta \in \left[0, \frac{\pi}{2}\right]$ denote the angle between P_1P_2 and $P_i\mathbf{u}_c$. According to central symmetry, $|P_1\mathbf{u}_c| = |P_2\mathbf{u}_c| = d$, then the distance from P_i to the pair of sides is

$$\min\{|P_iP_4|, |P_iP_5|\} = d - |P_i\mathbf{u}_c||\cos\beta| \leqslant d. \tag{8}$$

Therefore, the distance from P_i to any pair of parallel sides in Ω is no more than d, and $\rho(\mathbf{u}_c, \partial\Omega)$ is the maximum.

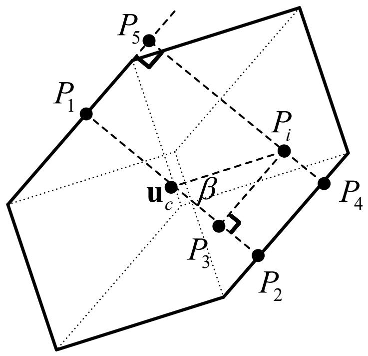

Figure 3. Schema of Ω.

Definition 1 (Degree of Controllability for Multicopters). The DoC for the multicopter system (3) is defined as

$$\sigma(\mathbf{d}) \triangleq \frac{\rho(\mathbf{d}, \partial\Omega)}{\rho(\mathbf{u}_c, \partial\Omega)}, \tag{9}$$

where $\rho(\mathbf{d}, \partial\Omega)$ is the ACAI of the multicopter system. From Definition 1, we can see that $\rho(\mathbf{d}, \partial\Omega) = \sigma \cdot \rho(\mathbf{u}_c, \partial\Omega)$.

According to (7), $\rho(\mathbf{d}, \partial\Omega) \leqslant 0$ if and only if the multicopter system is uncontrollable. For the sake of simplicity, let

$$\sigma = 0, \text{ if } \rho(\mathbf{d}, \partial\Omega) \leqslant 0. \tag{10}$$

Then, $\sigma = 0$ when the multicopter system (3) is uncontrollable. According to Lemma 1, (9) and (10), the following theorem holds.

Corollary 2. For the system in (3), the DoC satisfies $\sigma \in [0,1]$.

3.2.2. Input-dependent domain of attraction

Based on the defined DoC σ above, an input-dependent domain of attraction will be defined to help demonstrate the stability performance of the closed-loop system with the controller.

The input-dependent domain of attraction of the equilibrium of the system (3) is denoted by $\mathscr{S}$ for all disturbances. And mathematically, its definition is

$$\mathscr{S} = \left\{\mathbf{d} \middle| \lim_{t\to\infty} \mathbf{x}(t, \mathbf{u}, \mathbf{d}) \to 0, \mathbf{u} = C(t, \mathbf{x}) \in \Omega, \mathbf{d} \in \Omega\right\} \tag{11}$$

where $\mathbf{x}(t, \mathbf{u}, \mathbf{d})$ is the solution to the dynamic equation (3) subject to controller C and distrubance $\mathbf{d}$. Only the distrubance $\mathbf{d}$ satisfies $\sigma(\mathbf{d}) > 0$, namely $\mathbf{d} \in \Omega$, are considered since the system is uncontrollable if $\sigma(\mathbf{d}) \leqslant 0$. So it is obvious that $\mathscr{S} \subset \Omega$ (shown in Figure 4) and within the distance $\mathbf{d} \in \mathscr{S}$, the controller is capable of steering the state of the system $\mathbf{x}$ to origin.

The domain $\mathscr{S}$ is difficult to estimate because some flight controllers are proprietary or can be accessed only partially. Alternatively, it is easier to estimate the null controllable region. So, we hope to use a scaling-down and conservative, controllable region to replace $\mathscr{S}$ for safety measures. Before getting into the region, the safety threshold σ_{th} is defined as follows.

Definition 2 (Safety Threshold). The safety threshold of the system in (3) is defined as

$$\sigma_{th} \triangleq \sup \sigma(\mathbf{d}), \mathbf{d} \notin \mathscr{S}. \tag{12}$$

From the definition in (12), σ_{th} is determined by the controller $\mathbf{u} = C(t, \mathbf{x})$. And according to the definition in (11), the closed-loop system is stable if $\sigma \geqslant \sigma_{th}$. Then, we introduce the new scaling-down controllable region $\mathscr{C}_{\sigma_{th}}$ concerning control, defined as:

$$\mathscr{C}_{\sigma_{th}} \triangleq \{\mathbf{d} | \sigma(\mathbf{d}) \geqslant \sigma_{th}\}. \tag{13}$$

The value σ_{th} can be considered a minimum DoC to ensure stability. Then, the set $\mathscr{C}_{\sigma_{th}}$ is designed within the domain of attraction $\mathscr{S}$ by offline test, which is expected to be as large as possible. Their relationship is shown in Figure 4.

To show the stability margin of the closed-loop system intuitively, an input-dependent safety measure is defined based on Definition 1 and Definition 2.

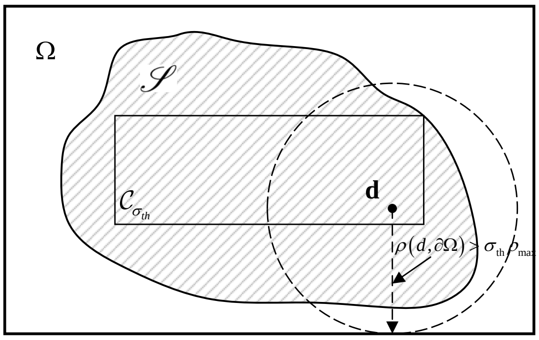

Figure 4. Relationship between the input-dependent domain of attraction and the null controllable region.

3.2.3. Definition of the input-dependent safety measure

Definition 3 (Input-Dependent Safety Measure). The input-dependent safety measure of the multicopter system in (3) is defined as

$$s \triangleq \frac{\sigma - \sigma_{th}}{1 - \sigma_{th}}, \tag{14}$$

where $\sigma_{th} < 1$ is the safety threshold of the closed-loop system (3) with the control strategy $\mathbf{u} = C(t, \mathbf{x})$.

From Definition 3, we say that the multicopter is safe if $s \geqslant 0$ and is unsafe otherwise. As $\sigma \in [0, 1]$, one has

$$s \in \left[\frac{-\sigma_{th}}{1 - \sigma_{th}}, 1 \right]. \tag{15}$$

Now, the stability of the multicopter system can be indicated by the input-dependent measure s. In order to clarify, Let M1, M2, and M3 denote the working mode of a multicopter when the system (4), (5) and (6) are considered, respectively. And let s_1, s_2, and s_3 denote the measure of each system.

Algorithm 1 Threshold Value Determination

1: Generate the disturbance grid set $\Xi \subset \mathbb{R}^n$ of the disturbance $\mathbf{d}$. As $\mathbf{d} \in \mathscr{U}_d$, the constraint of d_i can be obtained as $d_i \in [d_{i,\min}, d_{i,\max}]$ where $i = 1, \cdots, n$ and $d_{i,\min}, d_{i,\max}$ are the minimum and maximum values of d_i, respectively. Suppose that $[d_{i,\min}, d_{i,\max}]$ is divided into n_d grid points, then $\mathscr{U}_d$ changes to $\Xi \subset \mathbb{R}^n$ with n_d^n points.
2: Compute the ACAI of the multicopter system (3) corresponding to each disturbance grid point in Ξ.
3: Compute the DoC σ of each disturbance grid point in Ξ, with the results denoted by set Λ.
4: Let $k = 0$, and $\Delta\sigma \in (0, 1]$.
5: **if** $k\Delta\sigma > 1$ **then**
6:     go to Step 14.
7: **end if**
8: Check the stability of the specified control strategy $\mathbf{u} = C(t, \mathbf{x})$ for all the disturbance grid points satisfying $1 - k\Delta\sigma \leq \sigma < 1 - (k-1)\Delta\sigma$, which is denoted by Ξ_k.
9: **if** the closed-loop system with the control strategy $\mathbf{u} = C(t, \mathbf{x})$ is stable at all the specified disturbance grid points in Ξ_k **then**
10:     Let $k = k + 1$ and go to Step 5
11: **else**
12:     go to Step 14.
13: **end if**
14: The safety threshold is obtained as $\sigma_{th} = 1 - (k-1)\Delta\sigma$.

3.3. Threshold value determination

As mentioned above, a safety threshold σ_{th} exists for the specified controller $\mathbf{u} = C(t, \mathbf{x})$, and the closed-loop system is stable if $\sigma \geqslant \sigma_{th}$. Although one may obtain the theoretical value of σ_{th} if the explicit expression of the controller $\mathbf{u} = C(t, \mathbf{x})$ is simple, σ_{th} can be challenging to compute theoretically because the controller is either complex or only partially accessible in practice. This paper obtains the safety threshold σ_{th} via numerical simulations and real flight experiments. By taking the lumped disturbance $\mathbf{d}$ into account, the computing procedure is given in Algorithm 1, where the larger the value of n_d and the smaller the value of $\Delta\sigma$ are, the more accurate the threshold σ_{th} is.

4. Application of the input-dependent control safety measure

This section uses the proposed measure for a switching control framework for multicopters and shows how safe the multicopter is.

4.1. Switching control framework

In cases where the multicopter under severe off-nominal conditions is uncontrollable, a degraded control strategy is adopted. The studies [21–23] examined a relaxed hover solution for multicopters where the multicopter may rotate at a constant velocity in hover by giving up control of the yaw angle (the yaw states are ignored). These strategies can now be integrated into the controller with an online estimator for the measure, resulting in a robust switching control system against off-nominal conditions.

Let's take the above three modes as an example. First, we need to monitor the measure results of each system. Then, the switching conditions among the three control modes are shown in Table 1.

Table 1. The transfer condition among three control modes.

Mode	s_1 of System (4)	s_2 of System (5)	s_3 of System (6)
M1	>0	>0	>0
M2	$\leqslant 0$	>0	>0
M3	$\leqslant 0$	$\leqslant 0$	>0

The diagram of the switching control framework is shown in Figure 5. In practice, the top-level guidance module or the pilots on the ground gives the reference signal $\mathbf{x}_c$. Now, lots of studies have been conducted on the nominal control of multicopters; see, for example, [1, 2] and the references therein. To make this paper more extensible, the nominal control strategy in the framework is not specified.

In practice, many kinds of disturbance observers (such as the Kalman Filter) can be used to estimate disturbances based on the dynamic model shown in (3). If a Kalman filter is used to estimate the disturbance, then the estimated disturbance covariance can be used to obtain confidence for $\hat{\mathbf{d}}$. The ACAI is obtained according to the computation procedure given in [13] and the toolbox. Based on the ACAI, the input-dependent safety measure of the system is obtained according to Definition 3.

The measure can tell the autopilots whether it is necessary to switch to the degraded controllers and tell ground-based pilots the safe state of the multicopter. The ground-based pilots can help land the multicopter before the LOC accident occurs if necessary. The measure can be applied in the following scenarios:

i. Before a mission starts, the ground-based pilot can evaluate the safety based on a short-duration flight. Excessive payload and propulsor faults are checked based on the measure results.

ii. In the case of high winds, the ground-based pilots or onboard autopilots land the multicopter immediately if the measure approaches a sufficiently small value before the multicopter becomes unstable.
iii. In the event of sudden severe conditions, a ground-based pilot cannot predict the safe state based on the measure history or make a safety decision. At this time, the multicopter will try to land automatically in a degrading way. Otherwise, multicopter LOC will occur.

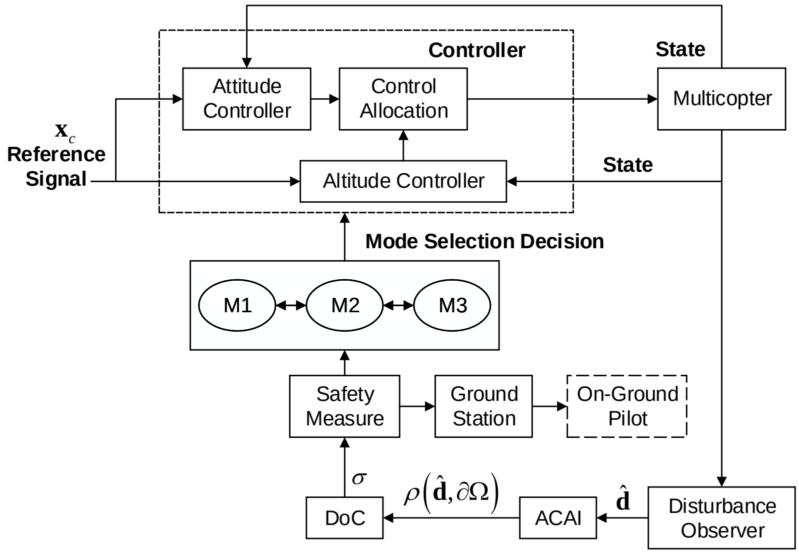

Figure 5. Switching control framework.

4.2. *Closed-loop stability statement*

According to Figure 5, the multicopter can switch between M1 and M2 or M2 and M3 to ensure safety. In practice, if the lumped disturbance **d** makes the multicopter switch from M1 to M2, the flight conditions are unsafe for the mission. If the disturbance makes the multicopter switch from M2 to M3, then the multicopter is unsafe and should land immediately. To prevent chattering, the average dwell time for each mode is defined to ensure the stability of the switched system [24].

5. Simulation and experiments

Both numerical and experimental results are given in this section to show the effectiveness of the proposed measure. Concretely, a hexacopter subject to propulsor faults is used to show the effectiveness of the proposed measure and switching control framework. Several real flight experiments based on a quadcopter platform are carried out to show the effectiveness of the input-dependent safety measure.

Under the proposed framework, off-nominal behaviors, such as additional payloads, propulsor degradation, and unacceptable wind disturbances, are all lumped together as disturbances. Therefore, only propulsor degradation (in the simulations) and additional payloads (in the experiments) are considered for simplicity and without loss of generality.

5.1. *Simulations and results*

Here, a traditional hexacopter with a symmetric configuration (see [13] for the detailed parameters of the hexacopter) is considered to show the effectiveness of the proposed measure and the switching control framework. The simulation model of the hexacopter is constructed and consists of three main modules:

i. two control strategies, namely, the nominal control strategy for M1 and the degraded control strategy for M2;
ii. a real-time estimator to obtain the measures s_1 and s_2;
iii. a switching control strategy based on the measure.

In the simulation, the hexacopter is controlled to operate 1 m above the ground ($h_c = 1$) and maintains a level state ($\phi_c = \theta_c = \psi_c = 0$).

To compute the ACAI $\rho(\mathbf{d}, \partial\Omega)$, a Kalman filter is used to estimate the lumped disturbance $\mathbf{d}$. Based on the estimated disturbance $\hat{\mathbf{d}}$, the value of the ACAI can be computed according to the procedure presented in [13]. Then, the DoC σ_1 and the measure s_1 can be computed based on the ACAI. Similarly, the lumped disturbance of the degraded system (5) can be estimated, and the DoC (denoted by σ_2) and the measure s_2 can be computed.

5.1.1. Threshold value determination

According to the procedure for computing the threshold value presented in Section 3.3., we set $n_d = 21$ and $\Delta\sigma = 0.1$, and perform simulations; the results are shown in Table 2 (where N_{total} is the total number of points and N_{stable} is the number of stable points). Table 2 shows that the altitude and attitude system controlled by the nominal control strategy is always stable if $\sigma_1 \geqslant 0.4$.

Table 2. Threshold value determination for σ_1.

σ_1	N_{total}	N_{stable}	Percentage
[0.9,1)	12	12	100%
[0.8,0.9)	90	90	100%
[0.7,0.8)	242	242	100%
[0.6,0.7)	478	478	100%
[0.5,0.6)	843	843	100%
[0.4,0.5)	1329	1329	100%
[0.3,0.4)	1865	1848	99%
[0.2,0.3)	2705	2380	88%
[0.1,0.2)	3190	2245	70%
[0,0.1)	183,727	1544	0.1%

Similarly, the degraded system controlled by a degraded control strategy is simulated and is always stable if $\sigma_2 \geqslant 0.4$ (details are omitted here). Then, we obtain the threshold value of the considered hexacopter as follows

$$\sigma_{1,th} = 0.4, \sigma_{2,th} = 0.4. \tag{16}$$

5.1.2. Simulation results

In the simulation, the hexacopter hovers, and the roll, pitch, and yaw angles are controlled. At the time $t = 5$ s, propulsor 2 fails, and the system switches to Mode M2 based on the switching control methodology. The simulation results are shown in Figure 6.

In Figure 6(a), the real-time position and attitude data are shown, with the multicopter in Mode M1 when no faults occur and then switching to Mode M2 after propulsor 2 fails. The real-time measures s_1 and s_2 are shown in Figure 6(b), from which it is observed that $s_1 < 0$ and $s_2 > 0$ after the failure of propulsor 2.

The results of the raw propulsor thrust $f_1, f_2, \cdots, f_6$ are shown in Figure 7, from which one can see that the thrust of propulsor 2 is zero after time $t = 5$ s. In Figure 6, the multicopter is pitching and rolling after the fault because the yaw channel controller is disabled.

To show how uncertainties in the estimation process affect the effectiveness of the recovery actions, estimation bias, different noise levels, and estimation phase delays are introduced into the system (4). Here, the bias is denoted by $\mathbf{d}_{\text{bias}}$, and the time delay is denoted by t_τ.

The standard deviation of the position and attitude sensor noises are denoted by χ_p and χ_a, respectively. The simulation results are shown in Figure 8.

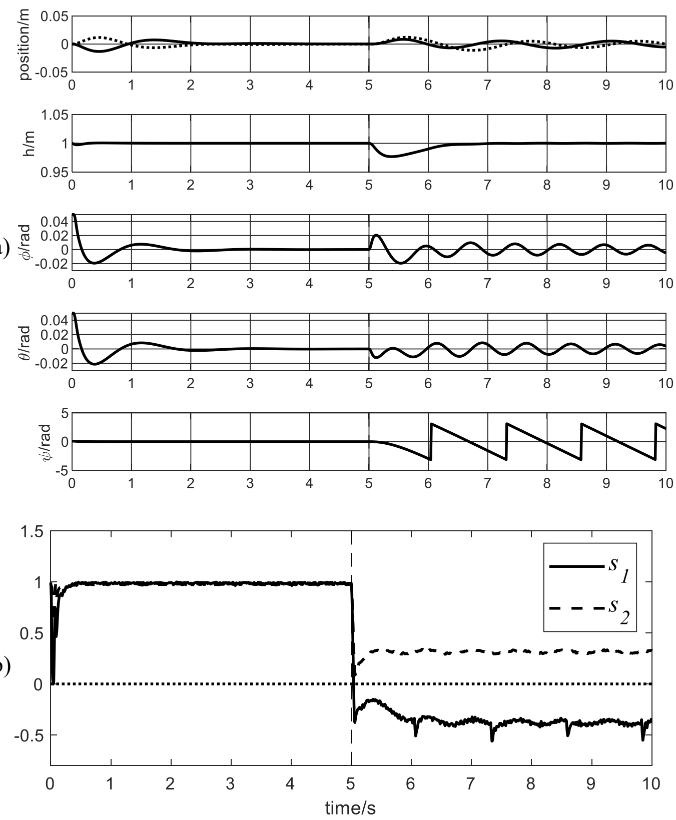

Figure 6. Simulation results: (a) position and attitude states. (b) real-time measures s_1 and s_2.

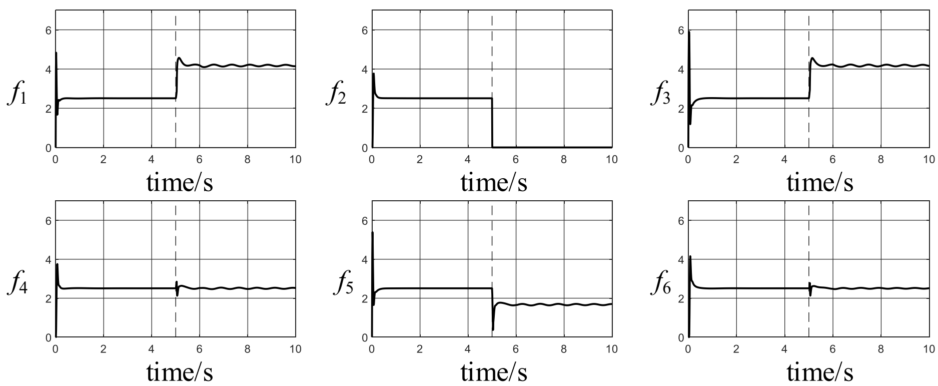

Figure 7. Simulation results of the raw propulsor thrust $f_1, f_2, \cdots, f_6$.

In Figure 8(a), the bias $\mathbf{d}_{\text{bias}} = \varepsilon_1 \mathbf{d}_0$ where $\mathbf{d}_0 \approx \begin{bmatrix} 21 & -1.4 & 0.9 & 0.6 \end{bmatrix}^{\mathrm{T}}$ and ε_1 is set to 0.05, 0.06, and 0.07. In Figure 8(b), the Kalman filter is designed based on given measurement noise $\chi_p = 0.1$ and $\chi_a = 0.01$, while the simulated measurement noises (denoted by χ_p' and χ_a') are $\chi_p' = (1+\varepsilon_2)\chi_p$, and $\chi_a' = (1+\varepsilon_2)\chi_a$. Here, ε_2 is set to 0.2, 0.4, and 0.6. In Figure 8(c), different delays (t_τ is set to 0.1s, 0.2s, 0.3s) are introduced into the disturbance estimation.

The results shown in Figure 8 indicate the following:

i. estimation bias will shift the estimated measure and may make the recovery action fail;
ii. different levels of noise do not affect the effectiveness of the recovery action;
iii. the delay term t_τ will delay the recovery action.

However, if the estimation bias and the delays are small enough, the recovery action based on the measure is effective.

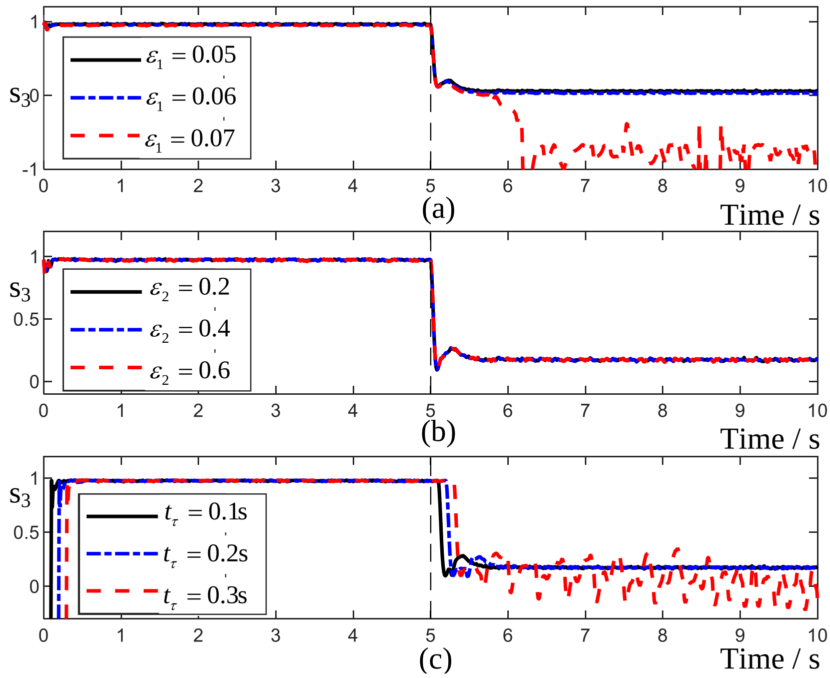

Figure 8. Effects of estimation bias, noise, and delays on the recovery actions: (a) $\varepsilon_2 = 0$, $t_\tau = 0$ s; (b) $\varepsilon_1 = 0$, $t_\tau = 0$ s; (c) $\varepsilon_1 = 0$, $\varepsilon_2 = 0$.

According to the simulation results, the fail-safe strategy based on the proposed measure is effective. In the following, experiments are carried out to show the effectiveness of the real-time measure estimator in the fail-safe strategy.

5.2. Experimental results

A quadcopter platform called Qball-X4 [25] (a quadcopter developed by Quanser shown in Figure 9) is used in the experiments to show that the measure can be used to monitor the safety state of the multicopter. The manufacturer of Qball-X4 offers a group of PID controllers for altitude and attitude control purposes.

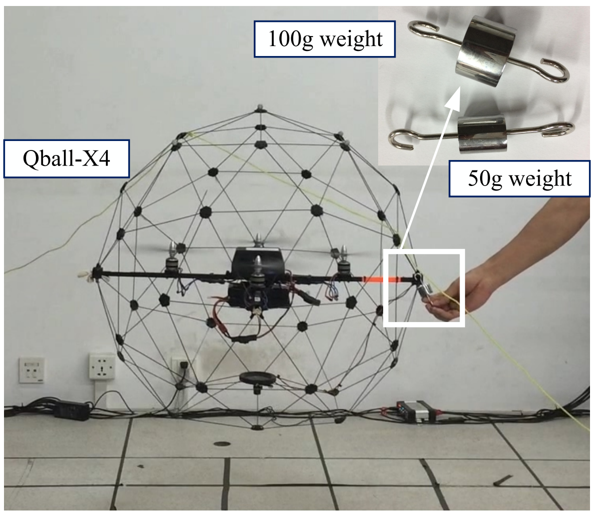

Figure 9. Quadcopter Qball-X4 and weights.

To obtain the safety threshold of Qball-X4, the Qball-X4 simulation model offered by the Quanser Company is modified slightly, and threshold value determination procedures are carried out. Here, the details are omitted, and the safety threshold of Qball-X4 is $\sigma_{th} = 0.3993$.

In the experiments, different weights are attached to the exact specified place, and the real-time measure of the altitude and attitude system, namely s_1, shows the safety state of the quadcopter. The maximum weight allowed by the quadcopter, $m_{\max} = 126$ g, is obtained via simulations to verify the experimental results. The primary purpose of these experiments is to verify the measure's effectiveness, which is used to show the real-time safety of the quadcopter and guide the autopilot to make decisions regarding safety (1 for safe and 0 for unsafe). These experiments are recorded in video and available online on YouTube; the experimental results are shown in Figure 10.

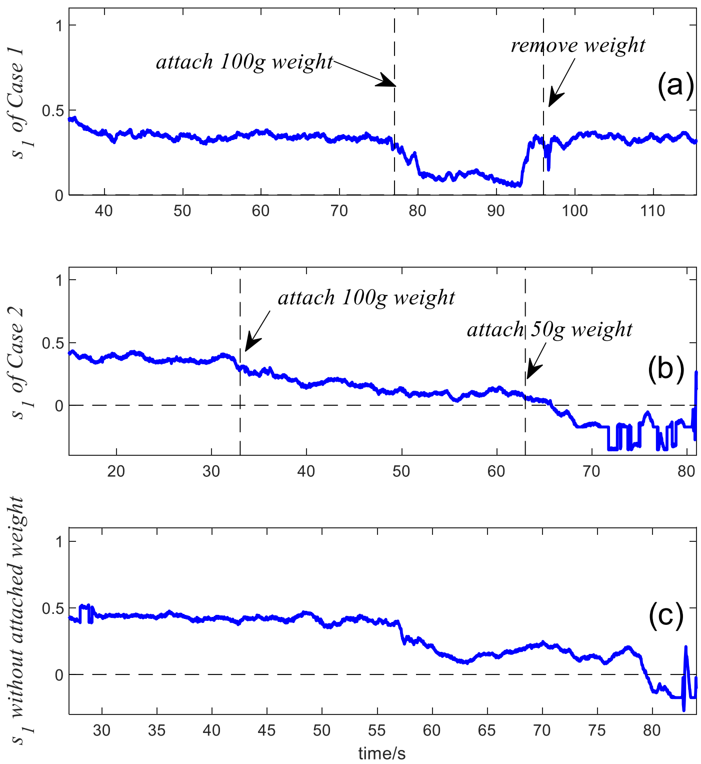

Figure 10. Experimental results: (a) Case 1: a 100-g weight was attached. (b) Case 2: weights totaling 150 g were attached. (c) effect of battery on s_1.

5.2.1. Case 1: a 100-g weight was attached to Qball-X4

Figure 10(a) shows the experimental results obtained when a 100-g weight was attached to a specified place on the multicopter. A 100-g weight was attached at time $t = 77$ s, and the aircraft was still safe with the PID controllers. Then, the 100-g weight was removed at time $t = 96$ s. The measure results in Figure10(a) show that Qball-X4 was always safe during the flight.

5.2.2. Case 2: weights totaling 150 g were attached to Qball-X4

In the second flight, multiple weights totaling 150 g were attached to the same part of Qball-X4, and the results are shown in Figure10(b). First, a 100-g weight was attached at time $t = 33$ s, with the aircraft remaining safe. Then, a 50-g weight was attached to the same place at time $t = 63$ s. The measure results in Figure10(b) show that Qball-X4 became unsafe after the 50-g weight was attached. From the video recording of this experiment, Qball-X4 became oscillating. The safety decision results are reasonable, as the maximum weight allowed is 126 g, while a total of 150 g was attached.

Figure10(a) and (b) show that the s_1 seems to drift a lot during a given experiment. A decrease in battery voltage causes this drift. If the battery voltage becomes low, each propulsor's maximum thrust decreases, equivalent to an extra weight being added to the multicopter. Figure10(c) shows the results when no weight was added to Qball-X4. The index s_1 is clearly decreased with the flight time. Thus, the measure proposed in this paper can reflect the effect of battery voltage change. From the above experiments, the measure proposed in this paper is practically effective. The measure can be used to monitor the real-time safety state of multicopters and to notify users whether a multicopter is safe to operate.

5.3. Discussion

In this paper, the model (5) or (6) are defined based on the equilibrium states that the multicopters can fly or hover or just not filp. And so is the framework that we proposed in the paper. That is to say, controllability analysis requires clarifying the equilibrium states and the model afterward. So, the method can still work for different types of multicopters or even other aircraft or vehicles if the equilibrium point and model are determined.

6. Conclusion

This paper investigated the safety measure problem for multicopters subject to off-nominal conditions. First, a new definition of the DoC was proposed for multicopters subject to control constraints and off-nominal conditions to show the available control authority of a multicopter. Then, an input-dependent safety measure was defined based on the new DoC to reflect the safety margin of multicopters. A step-by-step procedure was also provided to obtain the safety threshold, which was used to compute the measure. Besides, the proposed measure was used to guide the switching control of multicopters in a new switching control framework. Finally, the simulation results on a hexacopter and experimental results on a quadcopter demonstrated the effectiveness of the switching control framework and the measure proposed.

Acknowledgments

This work was supported by the National Natural Science Foundation of China under Grant 61973015.

Conflicts of interests

The authors declare no conflict of interest.

Authors' contribution

Conceptualization, Guangxun Du and Quan Quan; methodology & software, Guangxun Du and Gen Cui; validation, Quan Quan and Gen Cui; writing—original draft preparation, Guangxun Du and Quan Quan; writing—review & editing, Gen Cui and Quan Quan; visualization, Gen Cui; supervision, Zhiyu Xi, Yang Liu and Kai-Yuan Cai. All authors have read and agreed to the published version of the manuscript.

References

[1] Quan Q. *Introduction to Multicopter Design and Control*, Singapore: Springer, 2017.
[2] Mahony R, Kumar V, Corke P. Multirotor Aerial Vehicles: Modeling, Estimation, and Control of Quadrotor. *IEEE Robot. Autom. Mag.* 2012, 19(3):20–32.
[3] Belcastro CM, Foster JV, Newman RL, Groff L, Crider DA, *et al.* Aircraft Loss of Control: Problem Analysis for the Development and Validation of Technology Solutions. In *AIAA Guidance, Navigation, and Control Conference*, San Diego, CA, USA, 4–8 January 2016, 0092.
[4] Wang B, Zhang YM. An Adaptive Fault-Tolerant Sliding Mode Control Allocation Scheme for Multirotor Helicopter Subject to Simultaneous Actuator Faults. *IEEE Trans. Ind. Electron.* 2018, 65(5):4227–4236.
[5] Sun S, Wang X, Chu Q, de Visser C. Incremental Nonlinear Fault-Tolerant Control of a Quadrotor With Complete Loss of Two Opposing Rotors. *IEEE Trans. Robot.* 2021, 37(1):116–130.
[6] Hassan AM, Taha HE. Airplane loss of control problem: Linear controllability analysis. *Aerosp. Sci. Technol.* 2016, 55:264–271.
[7] Zhang Y, Jiang J. Bibliographical review on reconfigurable fault-tolerant control systems. *Annu. Rev. Control* 2008, 32(2):229–252.
[8] Badihi H, Zhang Y, Pillay P, Rakheja S. Fault-Tolerant Individual Pitch Control for Load Mitigation in Wind Turbines With Actuator Faults. *IEEE Trans. Ind. Electron.* 2021, 68(1):532–543.
[9] Guo J, Li Z, Li M. A Review on Prognostics Methods for Engineering Systems. *IEEE Trans. Reliab.* 2020, 69(3):1110–1129.
[10] Zio E. Some Challenges and Opportunities in Reliability Engineering. *IEEE Trans. Reliab.* 2016, 65(4):1769–1782.
[11] Pfifer H, Venkataraman R, Seiler P. Quantifying Loss-of-Control Envelopes via Robust Tracking Analysis. *J. Guid. Control Dyn.* 2017, 40(4):1042–1050.
[12] Batzel TD, Swanson DC. Prognostic Health Management of Aircraft Power Generators. *IEEE Trans. Aerosp. Electron. Syst.* 2009, 45(2):473–482.
[13] Du GX, Quan Q, Yang BX, Cai KY. Controllability Analysis for Multirotor Helicopter Rotor Degradation and Failure. *J. Guid. Control Dyn.* 2015, 38(5):978–985.
[14] Kalman RE, Ho YC, Narendra KS. Controllability of linear dynamical systems. *Contrib. Theory Differ. Equ.* 1963, 1(2):189–213.
[15] Li Y, Wang X, Huang R, Qiu Z. Actuator placement robust optimization for vibration control system with interval parameters. *Aerosp. Sci. Technol.* 2015, 45:88–98.
[16] Quan Q, Cui G, Du GX. Controllable probability and optimization of multicopters. *Aerosp. Sci. Technol.* 2021, 119:107162.
[17] Kang O, Park Y, sik Park Y, Suh MS. New Measure Representing Degree of Controllability for Disturbance Rejection. *J. Guid. Control Dyn.* 2009, 32(5):1658–1661.
[18] Xia Y, Yin M, Cai C, Zhang B, Zou Y. A new measure of the degree of controllability for linear system with external disturbance and its application to wind turbines. *J. Vib. Control* 2018, 24(4):739–759.
[19] Tahavori M, Hasan A. Fault recoverability for nonlinear systems with application to fault tolerant control of UAVs. *Aerosp. Sci. Technol.* 2020, 107:106282.
[20] Schneider T. Fault-tolerant multirotor systems. Master's thesis, ETH Zurich, 2011.
[21] Mueller MW, D'Andrea R. Stability and control of a quadrocopter despite the complete loss of one, two, or three propellers. In *2014 IEEE International Conference on Robotics and Automation (ICRA)*, Hong Kong, China, 2014, pp. 45–52.
[22] Du GX, Quan Q, Cai KY. Controllability Analysis and Degraded Control for a Class of Hexacopters Subject to Rotor Failures. *J. Intell. Robot. Syst.* 2015, 78(1):143–157.

[23] Lanzon A, Freddi A, Longhi S. Flight Control of a Quadrotor Vehicle Subsequent to a Rotor Failure. *J. Guid. Control Dyn.* 2014, 37(2):580–591.
[24] Lin H, Antsaklis PJ. Stability and Stabilizability of Switched Linear Systems: A Survey of Recent Results. *IEEE Trans. Automat. Contr.* 2009, 54(2):308–322.
[25] Zhang Y, Chamseddine A, Rabbath C, Gordon B, Su CY, *et al.* Development of advanced FDD and FTC techniques with application to an unmanned quadrotor helicopter testbed. *J. Franklin Inst.* 2013, 350(9):2396–2422.